Electronic Supplementary Material (ESI) for Materials Chemistry Frontiers.
This journal is © the Partner Organisations 2021

Supporting Information

Designed synthesis of CDs@Cu-ZIF-8 composites as excellent peroxidase mimics for assaying glutathione

Yufei Wang,[a] Mengke Wang,[b] Xiaoxue Wang,[a] Wenyan Ma,[a] Junxue Liu,[a] and Jiyang Li*[a]

[a] *State Key Laboratory of Inorganic Synthesis and Preparative Chemistry, College of Chemistry, Jilin University, Changchun 130012, P. R. China*

[b] *Department of Analytical Chemistry, College of Chemistry, Jilin University, Changchun, 130012, P. R. China*

*Corresponding author

E-mail address: lijiyang@jlu.edu.cn

Materials and Apparatus

Zinc oxide (ZnO), Copper nitrate ($Cu(NO_3)_2$), 2-methylimidazole (Hmin) and terephthalic acid (TA) were provided by Sinopharm Chemical Reagent Co. Ltd. (Shanghai, China). 3,3',5,5'-tetramethylbenzidine (TMB) and glutathione (GSH) were obtained from Aladdin (Shanghai, China). H_2O_2 (30%), H_3PO_4, NaAc, $CaCl_2$, KCl, and NaCl were purchased from Beijing Chemical Works Co. Ltd. (Beijing, China). Proline (Pro), arginine (Arg), D-serine (Ser), DL-tryptophan (Try), isoleucine (Iso), histidine (His), uric acid (UA), cysteine (Cys) and glutamine (Glu) were bought from Alfa (Shanghai, China). Human serum albumin (HAS) was bought from Psaitong. All the chemicals were obtained from commercial sources and used as received.

Power X-ray diffraction (XRD) data were recorded by Rigaku D/max-2550 diffractometer with a 2θ range of 4-40°, Cu Kα radiation (λ = 1.5418 Å), step time 1 s, and a step size of 0.02°. The transmission electron microscopy (TEM) and high resolution transmission electron microscopy (HR-TEM) images were carried out on an FEI Tecnai G2 S-Twin F20 transmission electron microscope in which the samples were dispersed in ethanol, following which the mixtures dropped in a carbon grid and dried at the room temperature. Scanning electron microscopy (SEM) was performed on a JEOL JSM-6700F SEM. UV-vis adsorption spectra and UV-vis diffuse reflectance spectra (DRS) were recorded on Shimadzu UV-2550 spectrophotometer and U-4100 spectrometer, respectively. The infrared (IR) absorption spectrum was taken with KBr pellets in the range of 4000 to 450 cm^{-1} using a Bruker FT-IR IFS-66 V/S spectrometer. A baseline correction was applied after measurement. Photoluminescence spectra were conducted by a HORIBA Scientific Fluoromax-4 spectrofluorometer. X-ray photoelectron spectroscopy (XPS) spectra were obtained on a Thermo ESCALAB250 spectrometer with monochromatized Al Kα excitation. All XPS peaks were calibrated according to the C 1s peak at 284.6 eV. Mott–Schottky plots were created by employing a three-electrode system in a 0.5 M $NaSO_4$ solution (PH=7.0), with a Pt foil counter-electrode and Ag/AgCl reference electrode, and the test were performed on a CHI 660D electrochemical workstation (Shanghai, China). Inductively coupled plasma analysis (ICP-AES) was measured by Perkin-Elmer Optima 3300 Dv.

The band-gap energies (E_g) are calculated according to Tauc plot:

$(\alpha \times h\nu)^{1/n} = A \times (h\nu - E_g)$

Among them, α is the absorption coefficient, A is the constant, hν is the photon energy, h is the

planck constant, v is the incident photon frequency, and E_g is the semiconductor forbidden band width (band gap), respectively. The system is a direct band gap and n=1/2.

According to the formula: hv=hc/λ, where c is the speed of light and λ is the wavelength of light and replace α with absorption value Abs. Plot with $(\alpha hv)^{1/n}$ and hv. Extrapolate the obtained straight-line to the abscissa axis, and the intersection point is E_g.

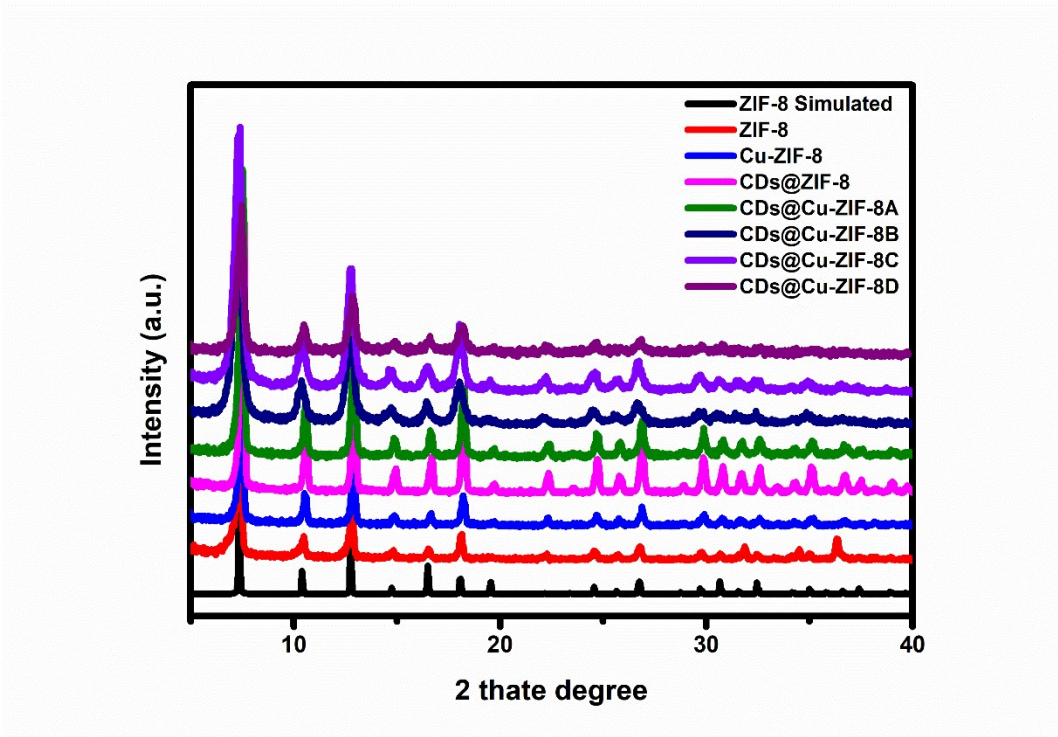

Fig. S1 XRD patterns of as-synthesized ZIF-8, Cu-ZIF-8, CDs@ZIF-8 and CDs@Cu-ZIF-8 composites.

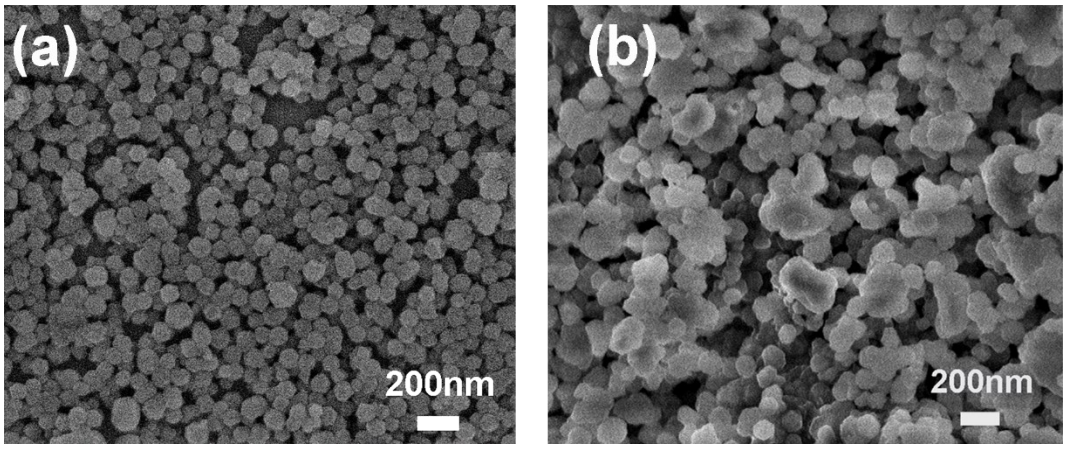

Fig. S2 SEM images of (a) Cu-ZIF-8 and (b) CDs@Cu-ZIF-8B

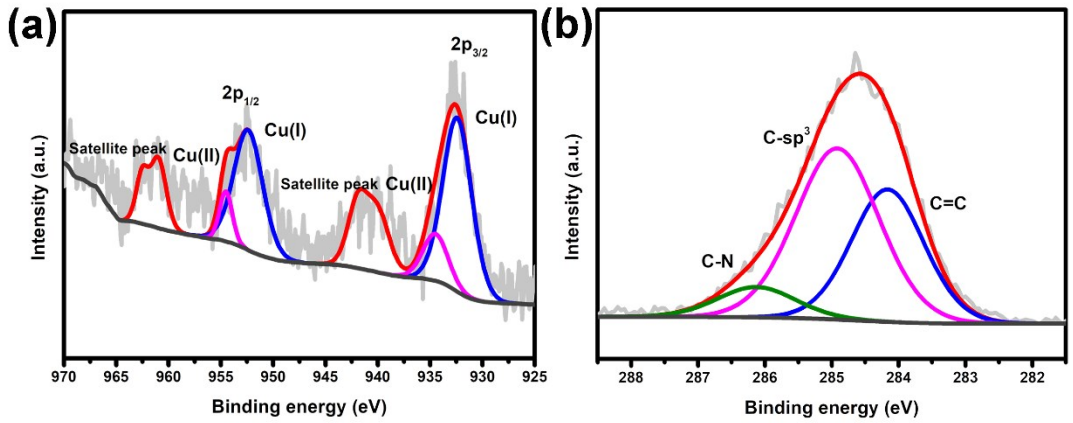

Fig. S3 The XPS spectra of Cu 2p and C s1 of Cu-ZIF-8.

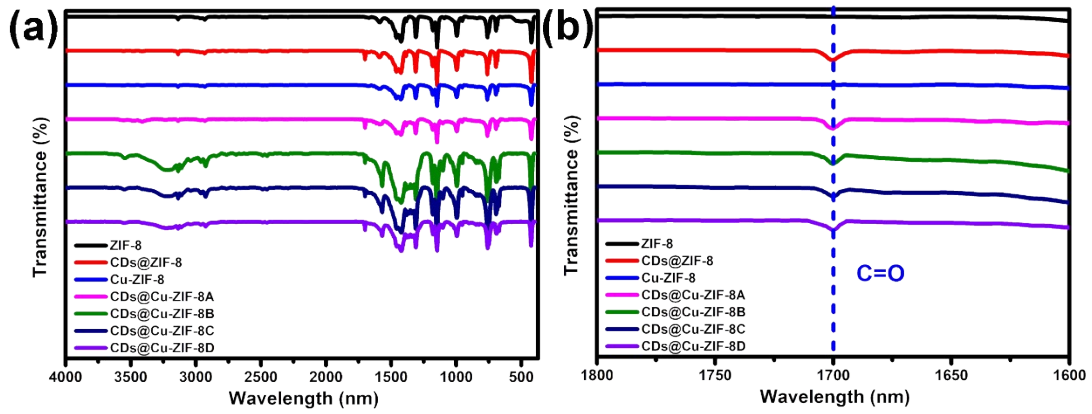

Fig. S4 (a) FT-IR spectra of ZIF-8, CDs@ZIF-8, Cu-ZIF-8 and CDs@Cu-ZIF-8 composites, and (b) the C=O peaks at 1700 cm^{-1}.

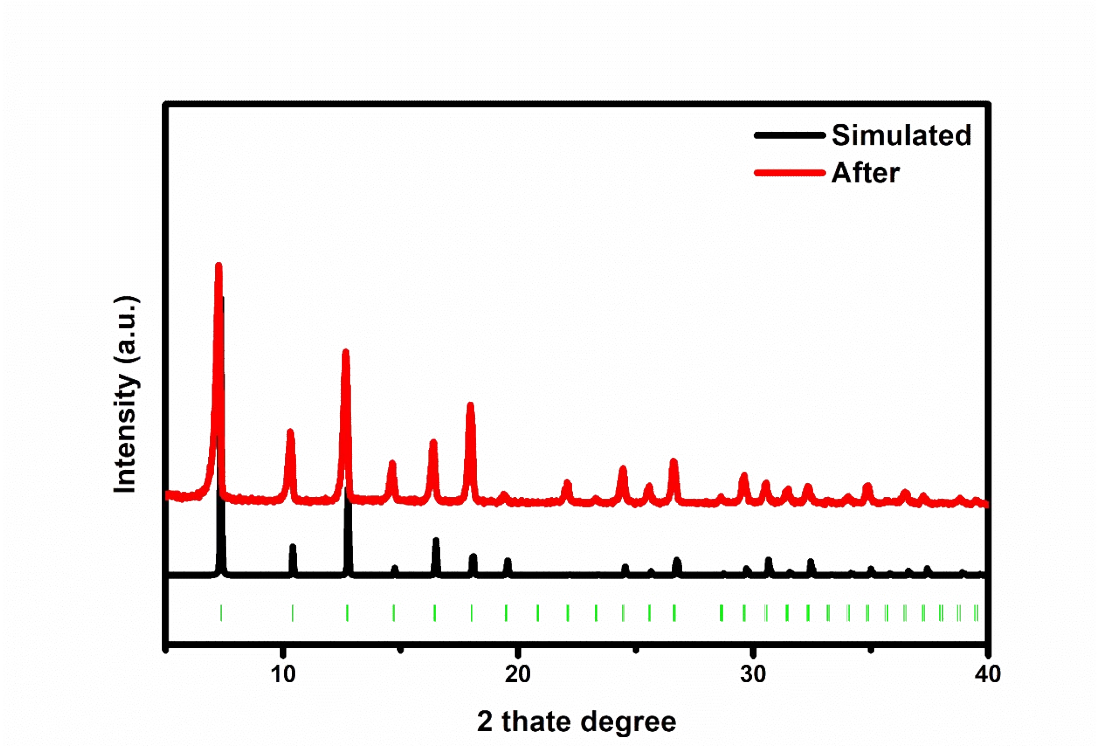

Fig. S5 XRD patterns of CDs@Cu-ZIF-8B after the catalytic reaction.

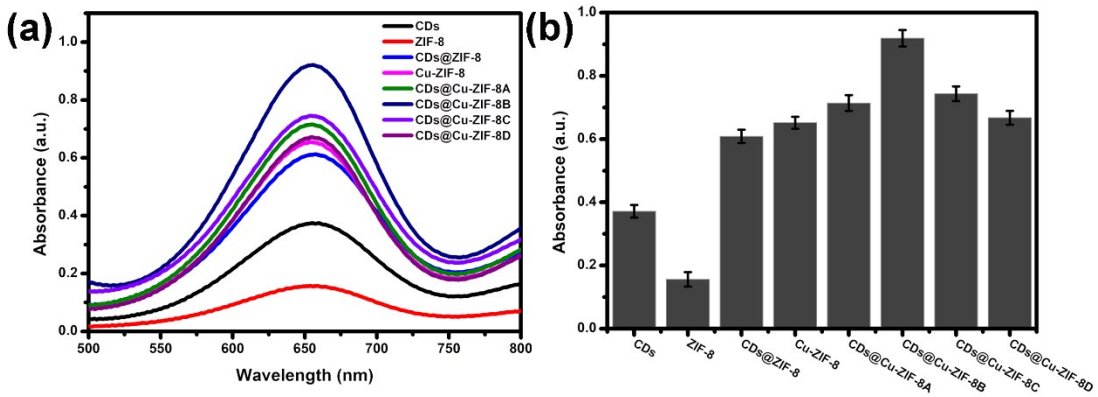

Fig. S6 (a) UV-vis absorption curves of CDs, ZIF-8, CDs@ZIF-8, Cu-ZIF-8 and CDs@Cu-ZIF-8， and (b) corresponding UV-vis absorption intensity at 652nm.

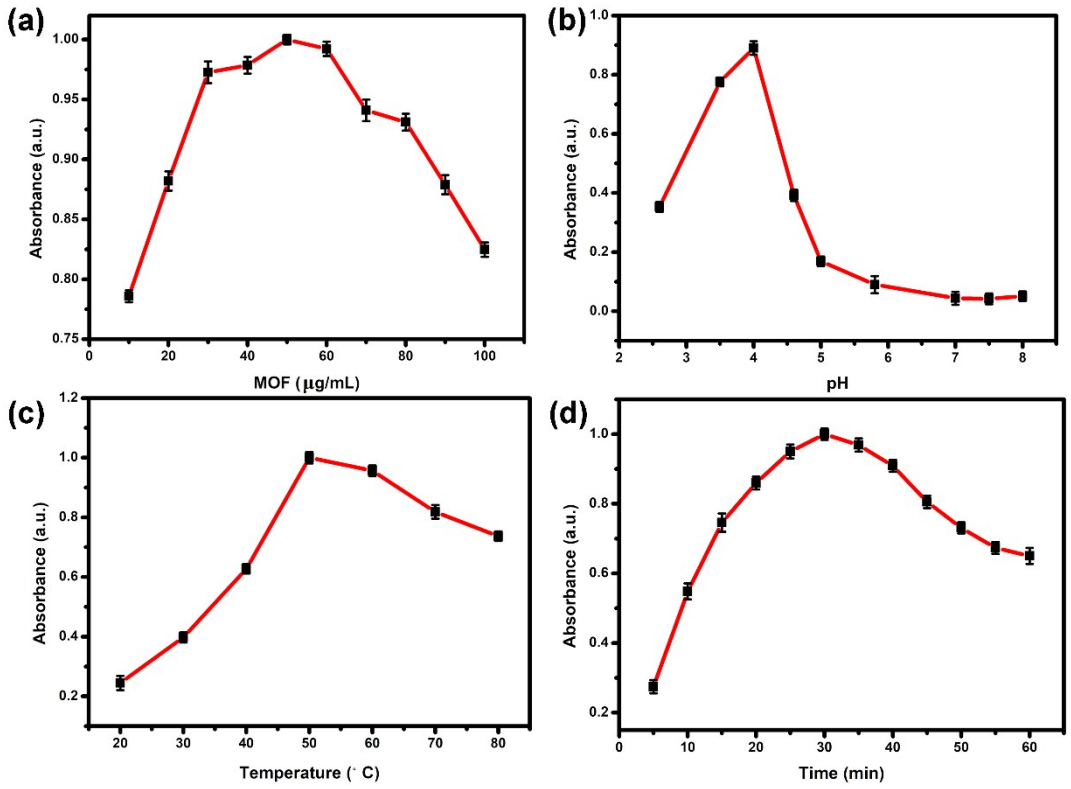

Fig. S7 UV-vis absorption at 652nm of (a) different amounts of CDs@Cu-ZIF-8B, (b) pH-, (c) temperature-, and (d) time-dependent activity of the reaction system under 0.05 mg/mL CDs@Cu-ZIF-8B, 0.3 mM TMB and 2.0 mM H_2O_2 in 0.20 M acetate buffer (pH = 4.0).

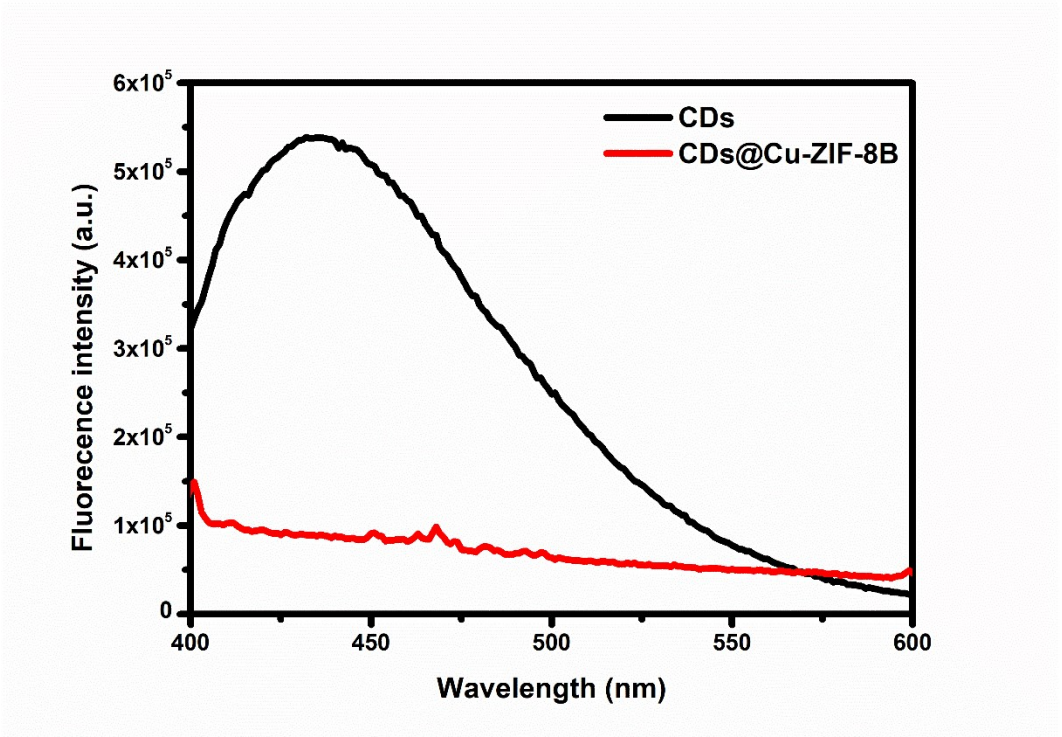

Fig. S8 Fluorescence spectra of CDs and CDs@Cu-ZIF-8B.

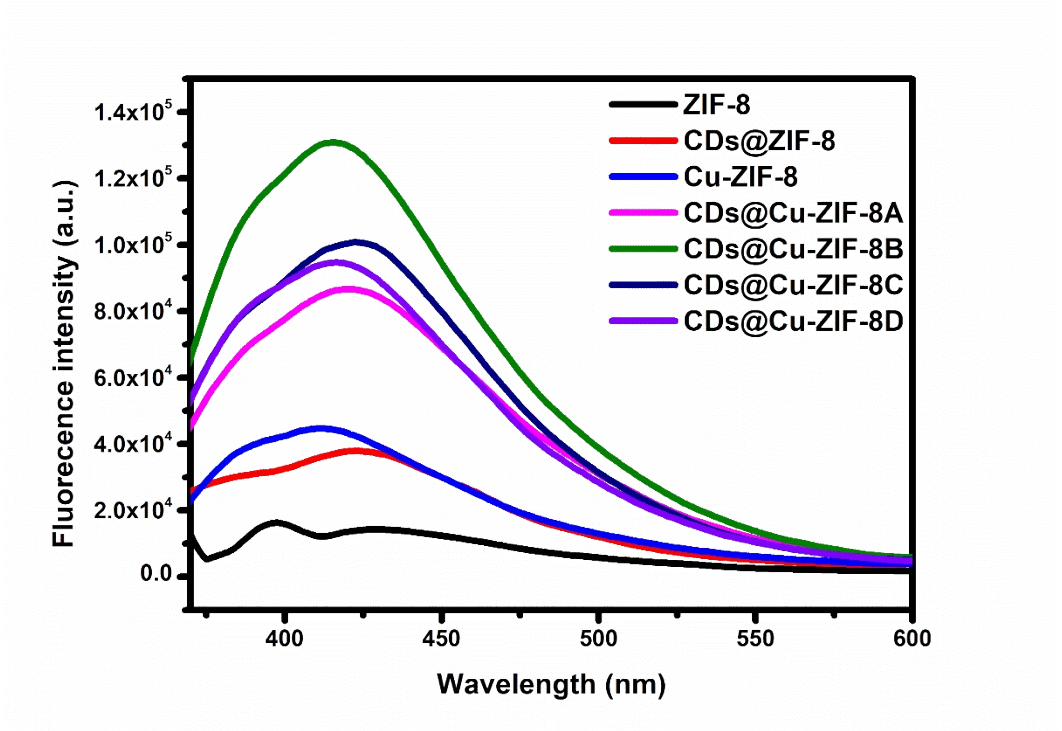

Fig. S9 Fluorescence spectra of TA (0.5 mM) and H_2O_2 (50 mM) with ZIF-8, CDs@ZIF-8, Cu-ZIF-8 and CDs@Cu-ZIF-8 composites of 0.5 mg/mL, respectively. The excitation wavelength was set to 314 nm.

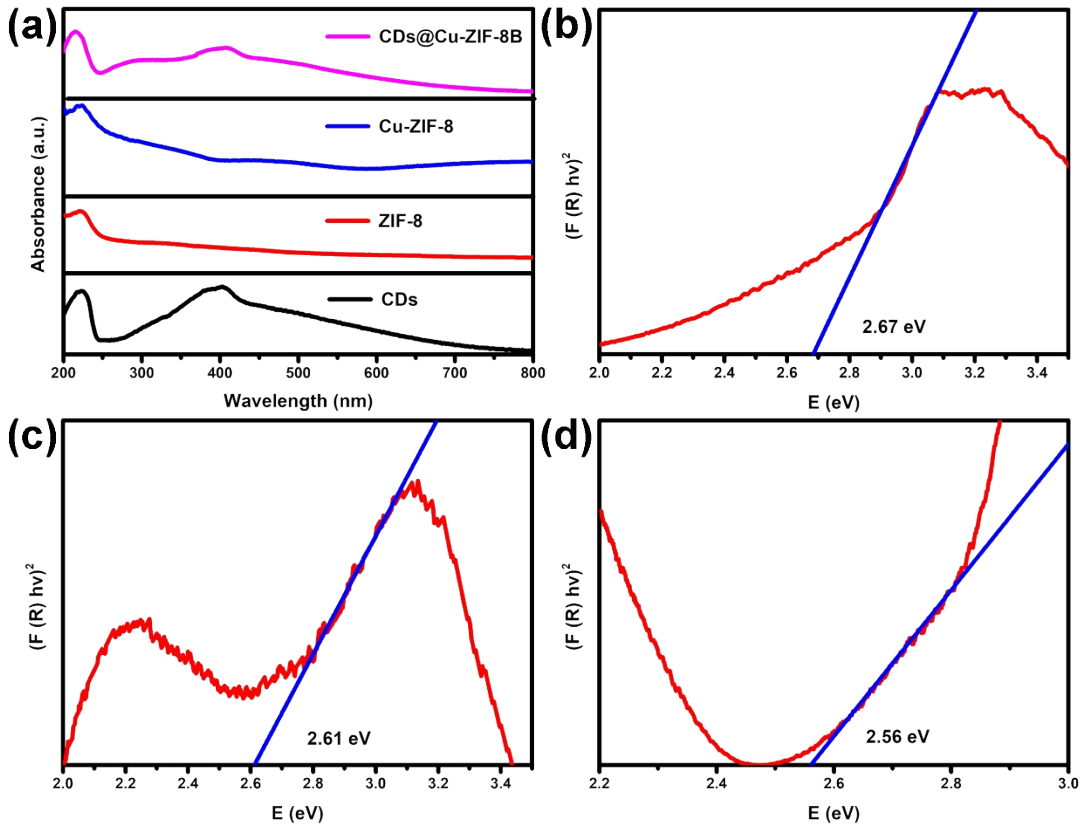

Fig. S10 (a) UV-Vis diffuse reflectance spectra of CDs, ZIF-8, Cu-ZIF-8 and CDs@Cu-ZIF-8B. The corresponding Tauc plot for (b) CDs, (c) Cu-ZIF-8, and (d) CDs@Cu-ZIF-8B, respectively.

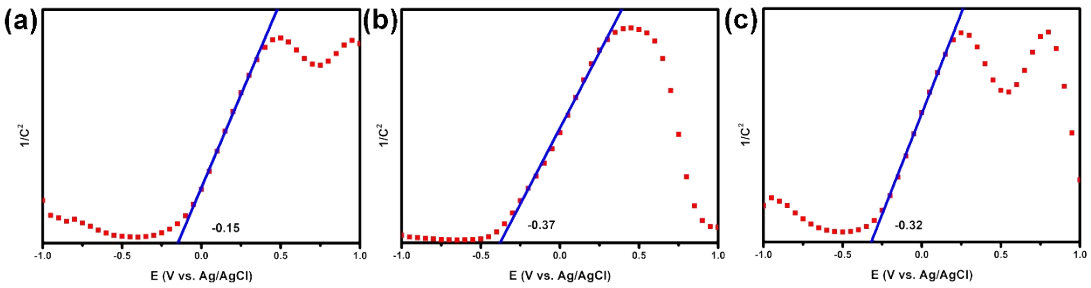

Fig. S11 Mott−Schottky plots for (a) CDs, (b) Cu-ZIF-8 and (c) CDs@Cu-ZIF-8B in 0.2 M Na_2SO_4 aqueous solution and the potential is vs. Ag/AgCl.

Table S1 Surface ratio of Cu(I) to Cu(II) calculated based on XPS result

Samples	Cu(I):Cu(II)
Cu-ZIF-8	91:9
CDs@Cu-ZIF-8B	89:10

Table S2 Comparison of the kinetic parameters (K_m and V_{max}) of various peroxidase-like mimics

	K_m(mM)		**V_{max}(10^{-8}M s^{-1})**		
	TMB	**H_2O_2**	**TMB**	**H_2O_2**	
N/S CDs	0.0765	0.0488	0.3096	0.6799	[1]
CB-CQDs	0.83	0.70	5.13	4.09	[2]
CQDs	0.427	0.244	4.29	22.2	[3]
ZIF-67	13.69	3.52	0.35	0.28	[4]
Cu-MOF	2.56	4.34	\	\	[5]
H_2TCPP/$Co(OH)_2$/GO	0.207	26.96	7.23	5.03	[6]
MXene@NiFe-LDH	0.187	0.078	1.707	2.076	[7]
CF@CuAl-LDH	4.4	0.59	1.48	0.29	[8]
GOx@ZIF-8@Fe-PDA	0.21	0.09	0.74	0.30	[9]
Hemin/ZIF-8	0.024	65.08	0.91	4.20	[10]
[Cu(PDA)(DMF)]	0.169	28.6	2.19	3.16	[11]
$CuFe_2O_4$	2.26	0.50	2.07	2.61	[12]
Cu-$CuFe_2O_4$	0.69	0.087	16.87	32.18	[12]
Cu NCs	1.125	2.52	7.20	16.80	[13]
$Cu_{1.8}$S NPs	1.72	37.1	\	\	[14]
HRP	0.434	3.70	10.00	8.71	[15]
CDs@ZIF-8-a	0.232	0.737	1.59	1.22	Previous work [16]
CDs@Cu-ZIF-8B	0.160	0.232	0.201	0.202	This work

Table S3. Comparison of various peroxidase-like mimics for detection of GSH

	Linear range (μM)	LOD (μM)	Ref.
N/S CDs	0.20 -12.00	0.26	[1]
CB-CQDs	0.5–20	0.6	[2]
Cu-MOF	0-100	0.97	[5]
H_2TCPP/Co(OH)$_2$/GO	10–300	9.50	[6]
Cu-$CuFe_2O_4$	2.5–10	0.31	[12]
Cu NCs	1–150	0.89	[13]
$Cu_{1.8}S$ NPs	500–10000	60	[14]
CDs@ZIF-8-a	0-100	1.04	Previous work [16]
CDs@Cu-ZIF-8B	0-40	0.15	This work

References

[1] M. Tang, B. Zhu, Y. Wang, H. Wu, F. Chai, F. Qu, et al., Nitrogen- and sulfur-doped carbon dots as peroxidase mimetics: colorimetric determination of hydrogen peroxide and glutathione, and fluorimetric determination of lead(II), Mikrochim. Acta. 186 (2019) 604.

[2] C. Yuan, X. Qin, Y. Xu, X. Li, Y. Chen, R. Shi, et al., Carbon quantum dots originated from chicken blood as peroxidase mimics for colorimetric detection of biothiols, J. Photochem. Photobiol. A 396 (2020) 112529.

[3] D. Bano, V. Kumar, V.K. Singh, S. Chandra, D.K. Singh, P.K. Yadav, et al., A Facile and Simple Strategy for the Synthesis of Label Free Carbon Quantum Dots from the latex of Euphorbia milii and Its Peroxidase-Mimic Activity for the Naked Eye Detection of Glutathione in a Human Blood Serum, ACS Sustainable Chem. Eng. 7 (2018) 1923-1932.

[4] S. Wang, D. Xu, L. Ma, J. Qiu, X. Wang, Q. Dong, et al., Ultrathin ZIF-67 nanosheets as a colorimetric biosensing platform for peroxidase-like catalysis, Anal. Bioanal. Chem. 410 (2018) 7145-7152.

[5] J. Wang, W. Li, Y.Q. Zheng, Nitro-functionalized metal-organic frameworks with catalase mimic properties for glutathione detection, Analyst 144 (2019) 6041-6047.

[6] X. Zhao, K. Wu, H. Lyu, X. Zhang, Z. Liu, G. Fan, et al., Porphyrin functionalized Co(OH)$_2$/GO nanocomposites as an excellent peroxidase mimic for colorimetric biosensing, Analyst 144 (2019)

5284-5291.

[7] H. Li, Y. Wen, X. Zhu, J. Wang, L. Zhang, B. Sun, Novel Heterostructure of a MXene@NiFe-LDH Nanohybrid with Superior Peroxidase-Like Activity for Sensitive Colorimetric Detection of Glutathione, ACS Sustainable Chem. Eng. 8 (2019) 520-526.

[8] L. Wu, G. Wan, S. Shi, Z. He, X. Xu, Y. Tang, et al., Atomic layer deposition-assisted growth of CuAl LDH on carbon fiber as a peroxidase mimic for colorimetric determination of H_2O_2 and glucose, New J. Chem. 43 (2019) 5826-5832.

[9] Z. Zhao, T. Lin, W. Liu, L. Hou, F. Ye, S. Zhao, Colorimetric detection of blood glucose based on GOx@ZIF-8@Fe-polydopamine cascade reaction, Spectrochim. Acta, Part A 219 (2019) 240-247.

[10] D. Li, S. Wu, F. Wang, S. Jia, Y. Liu, X. Han, et al., A facile one-pot synthesis of hemin/ZIF-8 composite as mimetic peroxidase, Mater. Lett. 178 (2016) 48-51.

[11] J. Wang, Y. Hu, Q. Zhou, L. Hu, W. Fu, Y. Wang, Peroxidase-like activity of metal-organicfFramework [Cu(PDA)(DMF)] and its application for colorimetric detection of dopamine, ACS Appl. Mater. Interfaces 11 (2019) 44466-44473.

[12] F. Xia, Q. Shi, Z. Nan, Facile synthesis of Cu-$CuFe_2O_4$ nanozymes for sensitive assay of H_2O_2 and GSH, Dalton Trans. 49 (2020) 12780-12792.

[13] C. Liu, Y. Cai, J. Wang, X. Liu, H. Ren, L. Yan, et al., Facile preparation of homogeneous copper nanoclusters exhibiting excellent tetraenzyme mimetic activities for colorimetric glutathione sensing and fluorimetric ascorbic acid sensing, ACS Appl. Mater. Interfaces 12 (2020) 42521-30.

[14] H. Zou, T. Yang, J. Lan, C. Huang, Use of the peroxidase mimetic activity of erythrocyte-like $Cu_{1.8}S$ nanoparticles in the colorimetric determination of glutathione, Anal. Methods 9 (2017) 841-846.

[15] M.S. Kim, J. Lee, H.S. Kim, A. Cho, K.H. Shim, T.N. Le, et al., Heme cofactor-resembling Fe-N single site embedded graphene as nanozymes to selectively detect H_2O_2 with high sensitivity, Adv. Funct. Mater. 30 (2019) 1905410.

[16] Y. Wang, X. Liu, M. Wang, X. Wang, W. Ma, J. Li, Facile synthesis of CDs@ZIF-8 nanocomposites as excellent peroxidase mimics for colorimetric detection of H_2O_2 and glutathione, Sens. Actuators, B (2020) 129115.